



Article

Emissions of CO₂, CH₄, and N₂O Fluxes from Forest Soil in Permafrost Region of Daxing'an Mountains, Northeast China

Xiangwen Wu, Shuying Zang *, Dalong Ma, Jianhua Ren, Qiang Chen and Xingfeng Dong

Heilongjiang Province Key Laboratory of Geographical Environment Monitoring and Spatial Information Service in Cold Regions, Harbin Normal University, Harbin 150025, China

* Correspondence: zsy6311@hrbnu.edu.cn; Tel.: +86-0451-8806-0689

Received: 4 June 2019; Accepted: 19 August 2019; Published: 20 August 2019



Abstract: With global warming, the large amount of greenhouse gas emissions released by permafrost degradation is important in the global carbon and nitrogen cycle. To study the feedback effect of greenhouse gases on climate change in permafrost regions, emissions of CO₂, CH₄, and N₂O were continuously measured by using the static chamber-gas chromatograph method, in three forest soil ecosystems (*Larix gmelinii*, *Pinus sylvestris* var. *mongolica*, and *Betula platyphylla*) of the Daxing'an Mountains, northeast China, from May 2016 to April 2018. Their dynamic characteristics, as well as the key environmental affecting factors, were also analyzed. The results showed that the flux variation ranges of CO₂, CH₄, and N₂O were $7.92 \pm 1.30 \sim 650.93 \pm 28.12$ mg·m⁻²·h⁻¹, $-57.71 \pm 4.65 \sim 32.51 \pm 13.03$ ug·m⁻²·h⁻¹, and $-3.87 \pm 1.35 \sim 31.1 \pm 2.92$ ug·m⁻²·h⁻¹, respectively. The three greenhouse gas fluxes showed significant seasonal variations, and differences in soil CO₂ and CH₄ fluxes between different forest types were significant. The calculation fluxes indicated that the permafrost soil of the Daxing'an Mountains may be a potential source of CO₂ and N₂O, and a sink of CH₄. Each greenhouse gas was controlled using different key environmental factors. Based on the analysis of Q₁₀ values and global warming potential, the obtained results demonstrated that greenhouse gas emissions from forest soil ecosystems in the permafrost region of the Daxing'an Mountains, northeast China, promote the global greenhouse effect.

Keywords: CO₂; CH₄; and N₂O fluxes; permafrost; forest soil; global warming potential; Q₁₀

1. Introduction

Global warming has become increasingly prominent. The average surface temperature of the earth has increased by 0.85 °C compared to that before the industrial revolution. This trend is expected to continue and reach an increase of 0.3~4.8 °C by the end of this century [1,2]. The latest analysis of observations from the World Meteorological Organization (WMO) and Global Atmosphere Watch (GAW) program showed that the concentration of CO₂ was 405.5 ± 0.1 ppm, that of CH₄ was 1859 ± 2 ppb, and that of N₂O was 329.9 ± 0.1 ppb in the atmosphere of 2017 [3]. Soil is the main source of greenhouse gas emissions. Almost 5~20% of CO₂, 15~30% CH₄, and 60~80% N₂O are emitted from soils to the atmosphere every year [4], which comprises a key contributor to climate warming. The concentration of greenhouse gas is closely related to the carbon and nitrogen cycles of ecosystems, and its "source-sink" relationship directly affects the response and feedback of ecosystems to climate change [5]. Therefore, the dynamics of three greenhouse gas fluxes have become an important aspect of global climate change research.

Permafrost is the result of energy exchange between the lithosphere and the atmosphere and is also an important part of the cryosphere. Global climate change directly affects both the

evolution and development of permafrost. Permafrost soils are large pools of carbon and nitrogen. Jorgenson et al. [6] estimated that one third of the world's carbon is fixed in soil active layers and permafrost, while 31~102 Pg of total nitrogen is stored in the top 3 m of permafrost [7]. Climate warming will increase the thickness of permafrost active layers, thus releasing the stored ancient carbon and water, and providing more living space and matrix for microorganisms. This increases the emission of greenhouse gases (e.g., CO₂, CH₄, and N₂O), which has a positive feedback effect on the global carbon or nitrogen cycle [8] and climate warming [9]. Therefore, understanding the characteristics of greenhouse gas flux in the permafrost region is of great scientific significance to recognize the carbon and nitrogen cycle of permafrost ecosystems or their response to global climate change.

Forest ecosystems are important players in the global carbon and nitrogen cycle process, and maintain 86% of the plant carbon pool and 73% of the soil carbon pool [10]. With global warming, the forest ecological environment changes, which changes the exchange of greenhouse gases between the atmosphere and forest soils, thus influencing the regional climate. Livesley et al. [11] and Jang et al. [12] found that the canopy, undergrowth litter, roots, and secretions of different tree species differ, resulting in differences in soil physical and chemical properties, microbial community composition and diversity, and changes greenhouse gas emission. Ju et al. [13] found that the soil ecosystem of coniferous forests was highly metabolized, and the CO₂ flux was significantly higher than that of broadleaf forests. In contrast, Leckie et al. [14] believed that coniferous forest litter was rich in refractory compounds, reducing the soil carbon and nitrogen mineralization rate, and resulting in a lower CO₂ flux. Wang et al. [15] reported that coniferous forests had thicker litter layer to intercept precipitation, which decreased the soil water content. Coniferous forest soil therefore had a stronger CH₄ absorption capacity than broadleaf forest soil. Castro et al. [16] believed that the difference in CH₄ fluxes between both forest types were not significant. The conclusions for soil N₂O flux in broadleaf forests and coniferous forests were also different. Butterbach-Bahl et al. [17] held that broadleaf forest soil was more likely to form an anaerobic environment and emit more N₂O. Several scholars have suggested that the N₂O emission of both forest types are similar, or that coniferous forests are slightly higher [18]. In summary, the effects of different forest types on the flux of CO₂, CH₄, and N₂O in soil remain unclear and need further investigation.

China is one of the world's three countries with permafrost regions. The permafrost area is about 220×10^4 km² [19]. Northeast China, in which the Xing'an-Baikal permafrost develops (approximately 39×10^4 km²), is one of the main distribution areas of permafrost at high latitudes in China, and is to the south of the most prominent part of the Eurasian high-latitude permafrost region [20]. The Daxing'an Mountains area is an important forestry base in China, with a forest coverage rate of 84.32%, which is significantly affected by human activities and climate warming. At present, research on greenhouse gases in Northeast China mainly includes in situ monitoring or indoor simulated incubation experiments, and mostly concentrates on arable land [21,22] or peat swamp wetlands [23,24]. Relatively few studies have addressed greenhouse gas fluxes of forest soils in the permafrost region of the Daxing'an Mountains, and quantitative assessment has not been conducted. This study continuously monitored (from May 2016 to April 2018) the dynamics of greenhouse gas fluxes in different forest types in the permafrost region of the Daxing'an Mountains. The effects of soil temperature, moisture, and other physical and chemical properties on CO₂, CH₄, and N₂O emissions were investigated, and the global warming potential (GWP) and Q₁₀ were evaluated. The purpose is to assess the greenhouse effect of greenhouse gases, released as a result of permafrost degradation in the Daxing'an Mountains, and provides a basis for the study of carbon and nitrogen budget in the Daxing'an Mountains' forest ecosystem.

2. Materials and Methods

2.1. Study Site

The study site was situated in the experimental area of the Mohe Forest Ecosystem National Positioning Observation and Research Station in Heilongjiang province ($53^{\circ}17' \sim 53^{\circ}30' \text{ N}$, $122^{\circ}06' \sim 122^{\circ}27' \text{ E}$) (Figure 1). The experimental area is located in the permafrost area of the Daxing'an Mountains, with low hills at an average elevation of 300~500 m. It is controlled by a cold temperate continental monsoon climate with an annual average temperature of -3.3°C and precipitation of 442.95 mm (monitored in 2016 and 2017). In this region, 66.47% of the precipitation is concentrated in summer (from June to August). Furthermore, the soil activity layer freeze-thaw period lasts for about half a year (from mid-April to mid-October), which is slightly longer than the snowpack cover time (from late October to early April). The annual sunshine hours are 2377~2625 h, with an annual total solar radiation of $402 \sim 448 \text{ kJ cm}^{-2}$, and $\geq 10^{\circ}\text{C}$ annual accumulated temperature of $1436 \sim 2062^{\circ}\text{C}$. The zonal soil of the study site is dark brown forest soil. The vegetation in this area belongs to the southern extension of the Eurasian cold-temperate coniferous forest. The zonal vegetation is dominated species of *Larix gmelinii*. Other major species include *Betula platyphylla*, *Pinus sylvestris* var. *mongolica*, *Populus davidiana*, etc. Common plants include *Ledum palustre* var. *dilatatum*, *Rhododendron dauricum*, *Vaccinium uliginosum*, *Vaccinium vitis-idaea*, and *Pyrola incarnate*. Sample selection was based on representative and feasibility principles. After comprehensive investigation, the three most typical forest types in the permafrost region of the Daxing'an Mountains: *Larix gmelinii* forest (LF), *Pinus sylvestris* var. *mongolica* forest (PF), *Betula platyphylla* forest (BF) were selected. One $100 \text{ m} \times 100 \text{ m}$ fixed experimental block with similar site conditions was set in each forest type (LF, PF and BF), and a total of 3 experimental blocks were set. All acronyms such as LF, PF, and BF which applicable for all tables and all figures.

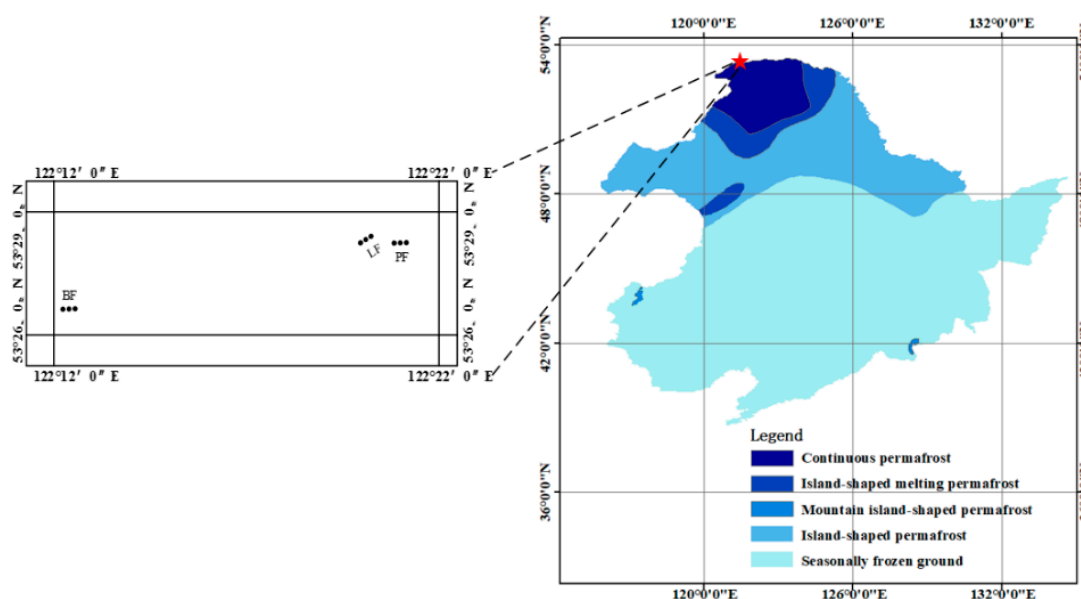


Figure 1. Study region location and sampling design. Black dot represents $5 \text{ m} \times 5 \text{ m}$ quadrat.

2.2. Measurement of CO_2 , CH_4 and N_2O Fluxes in Soil

Three $5 \text{ m} \times 5 \text{ m}$ quadrats were randomly distributed along the diagonal of each fixed experimental block ($100 \text{ m} \times 100 \text{ m}$) in each forest type, but each quadrat was separated by at least 20 m in order to collect greenhouse gas samples. A total of 9 quadrats were set in the three forest types. The static opaque chamber and gas chromatography method were adopted to monitor soil CO_2 , CH_4 , and N_2O gas fluxes in situ. The static chamber was mainly composed of the chamber and a stainless-steel base. Before sampling, the stainless-steel base with the water groove was buried in the quadrat one week

in advance, and was kept fixed during the whole monitoring period to reduce interference by the surrounding environment. The outside of the chamber was affixed with insulation material to decrease the temperature disturbance by the environment inside the box. Three holes were reserved at the top of the chamber to connect the fan power cable, the thermometer probe, and the sampling port, respectively. A 12-V battery-powered fan was installed in the chamber to evenly mix the gas.

In sunny weather, gas samples were collected during mid-morning (9:00~11:00 a.m., local time), which was used to represent one day of average flux [25], and once per week during the growing seasons (from May to September in 2016–2017) and once or twice per month during the non-growing seasons (from October 2016 to April 2017 and from October 2017 to April 2018). The aboveground plant inside the stainless-steel base was cut off 1 day before each sampling during the growing season, while natural snow accumulation was not treated during winter greenhouse gas collection. A medical syringe (60 mL), equipped with a three-way stopcock, was used to collect gas 0, 10, 20, and 30 min after the opaque chamber was sealed with water. When the temperature was below 0 °C, we brought our incubator to store water (300 mL of water per static chamber to water seal), and removed ice or water from the stainless-steel base after each experiment to facilitate the next sampling for water sealing. The samples were immediately transferred to a 200 mL gas sampling bag (Delin gas packing co., Dalian, China) and shipped back to the laboratory for analyzing by 7890B Gas Chromatography (7890B GC System, Agilent, CA, USA).

2.3. Soil Sampling and Analysis

In each quadrat (5 m × 5 m), five soil samples (0–15 cm) were randomly collected by removing the surface layer of the soil, and uniformly mixed into one subsample. Each time, 9 soil subsamples were collected from 3 fixed experimental blocks (100 m × 100 m), and total of 216 soil subsamples were collected during the observation period. The atmospheric pressure (BY-2003P barometer, Xieya Electronics Co., Beijing, China), air temperature (T_a), 10 cm soil temperature (T_{10}) (Delta TRAK portable thermometer, Delta TRAK, CA, USA) were measured simultaneously with soil sampling. All soil samples were shipped back to the laboratory in ziplock bags for the determination of soil moisture, bulk density (Bd), pH, ammonium nitrogen ($\text{NH}_4^+\text{-N}$), nitrate nitrogen ($\text{NO}_3^-\text{-N}$), total nitrogen (TN), and total organic carbon (TOC) (Table 1). Soil moisture was determined by the dry-weighing method. Soil bulk density was determined by the ring-knife method. Soil pH was determined in suspensions composed of 1:5 ratio of air-dried soil and deionized water using a PHSJ-3F pH meter (PHSJ-3F pH, Shanghai, China). Soil $\text{NH}_4^+\text{-N}$ and $\text{NO}_3^-\text{-N}$ were determined by extraction with potassium chloride solution-spectrophotometric method using a flow injection auto-analyzer (Skalar SAN++, The Netherlands) [26]. Soil TN was determined spectrophotometric using a flow injection auto-analyzer (Skalar SAN++, The Netherlands) [27]. Soil TOC was determined using the dry combustion method by TOC/TN analyzer (Multi C/N 3100, Jena, Germany) [28].

Table 1. The surface soil (0~15 cm) physicochemical properties in LF, PF, and BF (mean ± SD, $n = 216$).

Blocks	pH	Bd ($\text{g}\cdot\text{cm}^{-3}$)	$\text{NO}_3^-\text{-N}$ ($\text{mg}\cdot\text{kg}^{-1}$)	$\text{NH}_4^+\text{-N}$ ($\text{mg}\cdot\text{kg}^{-1}$)	TN ($\text{g}\cdot\text{kg}^{-1}$)	TOC ($\text{g}\cdot\text{kg}^{-1}$)	C/N
LF	5.53 ± 0.23a	1.01 ± 0.08a	1.57 ± 0.54ab	5.01 ± 0.91c	3.30 ± 0.97ab	52.22 ± 6.21ab	15.82ab
PF	5.57 ± 0.18a	1.05 ± 0.06a	1.31 ± 0.34b	6.67 ± 1.05b	2.91 ± 0.77b	48.36 ± 4.77b	16.62a
BF	4.65 ± 0.17b	0.71 ± 0.09b	2.10 ± 0.42a	10.23 ± 1.24a	4.16 ± 0.85a	58.50 ± 5.17a	14.06b

Note: Lowercase letters indicate differences in physical and chemical indicators between different forest types ($P < 0.05$).

2.4. Statistical Analysis

The gas flux was calculated according to the following equation [29]:

$$F = \frac{dc}{dt} \times \frac{M}{V_0} \times \frac{P}{P_0} \times \frac{T_0}{T} \times H \quad (1)$$

where F ($\text{mg}\cdot\text{m}^{-2}\cdot\text{h}^{-1}$) is the gas flux, dc/dt is the slope of the linear regression for the gas concentration gradient over time, M ($\text{g}\cdot\text{mol}^{-1}$) is the molecular mass of gas, P (Pa) is the atmospheric pressure in sampling site, T (k) is the temperature inside the chamber during sampling, H (m) is the height of chamber, V_0 ($\text{m}^3\cdot\text{mol}^{-1}$), P_0 (Pa) and T_0 (k), are the gas mole volume, atmospheric pressure under standard conditions, and absolute air temperature, respectively. A positive F -value means that there is a net emission of gas, and a negative value is the opposite.

The global warming potential (GWP) was calculated according to [30]:

$$\text{GWP} = F_{\text{CO}_2} + F_{\text{CH}_4} \times 25 + F_{\text{N}_2\text{O}} \times 298 \quad (2)$$

where F_{CO_2} , F_{CH_4} and $F_{\text{N}_2\text{O}}$ represent the greenhouse gas emission flux during the monitoring period ($\text{t}\cdot\text{hm}^{-2}$), 25 and 298 are the conversion factors of CH_4 and N_2O , respectively (for a 100 timeframe), to present GWP in $\text{t CO}_2 \text{ Eq}\cdot\text{ha}^{-1}$.

The following equation was established to calculate the temperature sensitivity of gas flux to the changes of T_{10} [31,32]:

$$F = ae^{bT} \quad Q_{10} = e^{10b} \quad (3)$$

where F is the gas flux, T is the soil temperature, coefficient a is the intercept of soil respiration when temperature is zero, coefficient b represents the temperature sensitivity of soil respiration, Q_{10} is the temperature sensitivity.

The differences in soil environment factors among all forests were compared using one-way ANOVA and Tukey's tests. The relationships of the soil greenhouse gas fluxes with soil temperature and moisture were assessed by regression analysis. The correlations between soil greenhouse gas fluxes and physical and chemical properties were analyzed by Pearson correlation with two tails. SPSS 20.0 (SPSS Inc., Chicago, IL, USA) was used for statistical analysis. All figures were drawn using OriginPro 2016 software (OriginLab Corp., Northampton, MA, USA.).

3. Results

3.1. The Temporal Variation of Soil CO_2 Fluxes across LF, PF, and BF

The temporal variations of soil CO_2 fluxes in the three forest types in the permafrost region of Daxing'an Mountains were basically exactly the same (Figure 2a). The whole monitoring period was characterized by emissions with significant seasonal variations. The soil CO_2 fluxes ranged from $7.92 \pm 1.30 \text{ mg}\cdot\text{m}^{-2}\cdot\text{h}^{-1}$ to $650.93 \pm 28.12 \text{ mg}\cdot\text{m}^{-2}\cdot\text{h}^{-1}$, and both were unimodal during the two monitoring periods. The majority of emissions were concentrated during the growing season (average fluxes $341.92 \pm 202.41 \text{ mg}\cdot\text{m}^{-2}\cdot\text{h}^{-1}$), while emissions were relatively low during the non-growing season (average flux $57.92 \pm 29.13 \text{ mg}\cdot\text{m}^{-2}\cdot\text{h}^{-1}$). PF soil CO_2 emissions reached a maximum in July ($650.93 \pm 28.12 \text{ mg}\cdot\text{m}^{-2}\cdot\text{h}^{-1}$), and LF and BF reached the maximum emissions in August ($629.8 \pm 33.91 \text{ mg}\cdot\text{m}^{-2}\cdot\text{h}^{-1}$, $536.27 \pm 22.36 \text{ mg}\cdot\text{m}^{-2}\cdot\text{h}^{-1}$, respectively). PF, LF, and BF reached minimum fluxes of $7.92 \pm 1.3 \text{ mg}\cdot\text{m}^{-2}\cdot\text{h}^{-1}$ (February), $10.27 \pm 3.92 \text{ mg}\cdot\text{m}^{-2}\cdot\text{h}^{-1}$ (February), and $15.63 \pm 2.31 \text{ mg}\cdot\text{m}^{-2}\cdot\text{h}^{-1}$ (March), respectively. The average annual flux of CO_2 in three forest types followed PF ($291.76 \text{ mg}\cdot\text{m}^{-2}\cdot\text{h}^{-1}$) > LF ($273.84 \text{ mg}\cdot\text{m}^{-2}\cdot\text{h}^{-1}$) > BF ($243.29 \text{ mg}\cdot\text{m}^{-2}\cdot\text{h}^{-1}$). The soil CO_2 fluxes in coniferous forest were higher than in broad-leaved forest, and PF soil CO_2 cumulative fluxes were significantly higher than BF (Table 2).

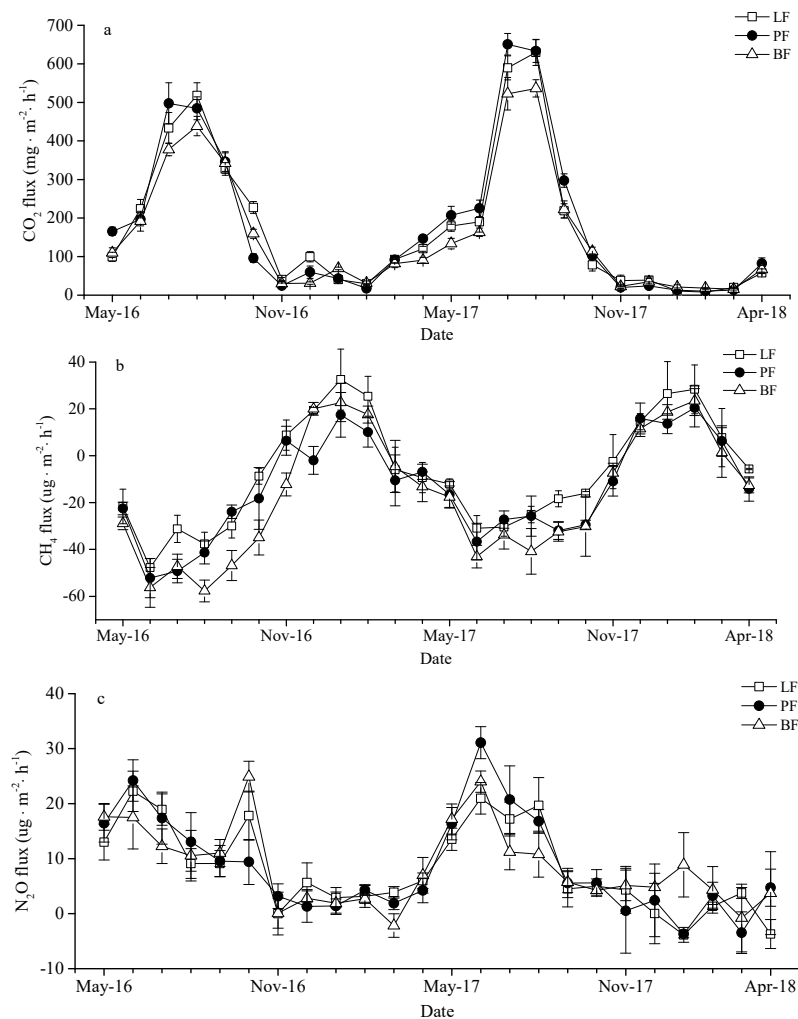


Figure 2. Temporal variation of soil CO₂ (a), CH₄ (b), and N₂O (c) fluxes in LF, PF, and BF.

Table 2. Average cumulative fluxes and GWP of greenhouse gases from LF, PF, and BF.

Blocks	CO ₂ (t·hm ⁻²)	CH ₄ (kg·hm ⁻²)	N ₂ O (kg·hm ⁻²)	GWP (t CO ₂ Eq·hm ⁻²)
LF	15.737 ± 1.14ab	−0.639 ± 0.19a	0.715 ± 0.14a	15.934 ± 1.18ab
PF	16.249 ± 0.38a	−1.208 ± 0.28ab	0.757 ± 0.02a	16.445 ± 0.38a
BF	13.876 ± 0.61b	−1.483 ± 0.40b	0.756 ± 0.03a	14.064 ± 0.61b

Note: Lowercase letters indicate differences in indicators between different forest types ($P < 0.05$).

3.2. The Temporal Variation of Soil CH₄ Fluxes across LF, PF, and BF

During the test, the three types of forest soil all showed CH₄ absorption fluxes (Figure 2b), with apparent seasonal fluctuations. The soil CH₄ fluxes had similar temporal variation in LF, PF, and BF, which showed increasing fluctuation from June to January of the following year, followed by a gradual decreased until June. The soil CH₄ fluxes ranged from $-57.71 \pm 4.65 \text{ ug}\cdot\text{m}^{-2}\cdot\text{h}^{-1}$ to $32.51 \pm 13.03 \text{ ug}\cdot\text{m}^{-2}\cdot\text{h}^{-1}$. During the growing season, all three types of forest soil absorbed CH₄; however, positive CH₄ fluxes were found in winter. The highest absorption for CH₄ fluxes from LF and PF were observed in June ($-47.76 \pm 3.9 \text{ ug}\cdot\text{m}^{-2}\cdot\text{h}^{-1}$, $-52.18 \pm 8.36 \text{ ug}\cdot\text{m}^{-2}\cdot\text{h}^{-1}$), while it was August for BF ($-57.71 \pm 4.65 \text{ ug}\cdot\text{m}^{-2}\cdot\text{h}^{-1}$). The peak fluxes from PF and BF occurred in February ($20.43 \pm 8.15 \text{ ug}\cdot\text{m}^{-2}\cdot\text{h}^{-1}$, $23.46 \pm 6.35 \text{ ug}\cdot\text{m}^{-2}\cdot\text{h}^{-1}$), and in January for LF ($32.51 \pm 13.03 \text{ ug}\cdot\text{m}^{-2}\cdot\text{h}^{-1}$). The average annual flux of CH₄ in LF, PF, and BF were $-19.33 \text{ ug}\cdot\text{m}^{-2}\cdot\text{h}^{-1}$, $-24.59 \text{ ug}\cdot\text{m}^{-2}\cdot\text{h}^{-1}$, and $-30.46 \text{ ug}\cdot\text{m}^{-2}\cdot\text{h}^{-1}$, respectively. The soil CH₄ absorption fluxes in broad-leaved forest were higher

than in coniferous forest, and BF soil CH₄ cumulative absorption fluxes were significantly higher than LF (Table 2).

3.3. The Temporal Variation of Soil N₂O Fluxes across LF, PF, and BF

The soil N₂O fluxes of the three forest types were largely consistent during the monitoring period of 2016~2018 (Figure 2c). The soil N₂O fluxes ranged from $-3.87 \pm 1.35 \text{ ug}\cdot\text{m}^{-2}\cdot\text{h}^{-1}$ to $31.1 \pm 2.92 \text{ ug}\cdot\text{m}^{-2}\cdot\text{h}^{-1}$ in LF, PF, and BF. Emissions during the non-growing season were at a relatively low value with a small amount of absorption and concentrated during the growing season. Soil N₂O fluxes showed a bimodal trend during 2016–2017, and a unimodal trend during 2017~2018. The maximum soil N₂O fluxes of LF ($22.25 \pm 3.66 \text{ ug}\cdot\text{m}^{-2}\cdot\text{h}^{-1}$) and PF ($31.1 \pm 2.92 \text{ ug}\cdot\text{m}^{-2}\cdot\text{h}^{-1}$) were recorded in June, and those for BF ($24.91 \pm 2.8 \text{ ug}\cdot\text{m}^{-2}\cdot\text{h}^{-1}$) in October. In contrast, the minimum absorption of N₂O fluxes were recorded in January (LF: $-3.87 \pm 1.35 \text{ ug}\cdot\text{m}^{-2}\cdot\text{h}^{-1}$, PF: $-3.68 \pm 0.68 \text{ ug}\cdot\text{m}^{-2}\cdot\text{h}^{-1}$) and March (BF: $-2.17 \pm 2.13 \text{ ug}\cdot\text{m}^{-2}\cdot\text{h}^{-1}$), respectively. The average annual flux of N₂O for PF ($13.33 \text{ ug}\cdot\text{m}^{-2}\cdot\text{h}^{-1}$) were higher than LF ($11.8 \text{ ug}\cdot\text{m}^{-2}\cdot\text{h}^{-1}$) and BF ($11.45 \text{ ug}\cdot\text{m}^{-2}\cdot\text{h}^{-1}$). The soil N₂O fluxes in coniferous forest were higher than in broad-leaved forest.

3.4. Cumulative Soil Greenhouse Gas Emissions and GWP

This study showed that the CO₂ accumulation fluxes of three forest types in the permafrost region of the Daxing'an Mountains dominated, followed by N₂O and CH₄ as absorption fluxes (Table 2). However, LF, PF, and BF showed the “source” of greenhouse gases. The global warming potential is to evaluate the relative impact of greenhouse gases on global climate change using CO₂ as a reference gas on a 100-year time scale. The radiation effects of CH₄ and N₂O were 25 times and 298 times that of CO₂, respectively [4]. The greenhouse gas GWP value of three forest types showed: PF > LF > BF (Table 2). The study clarified that the release of greenhouse gases from forest soils in the permafrost region of the Daxing'an Mountains has a positive effect on global warming, and the greenhouse gas GWP value of coniferous forests was higher than that of broad-leaved forests.

3.5. Effects of Environmental Factors on Soil Greenhouse Gas Fluxes

Soil temperature and moisture directly or indirectly affected the production and release of greenhouse gases. The correlations between gas fluxes and soil temperature were higher for CO₂ ($0.84 < R^2 < 0.89$, $P < 0.001$; Figure 3a) and CH₄ ($0.62 < R^2 < 0.76$, $P < 0.001$; Figure 3b) than for N₂O ($0.22 < R^2 < 0.35$, $P < 0.001$; Figure 3c). Soil moisture was positively correlated with CH₄ fluxes ($0.45 < R^2 < 0.7$, $P < 0.001$; Figure 3e), while CO₂ ($0.23 < R^2 < 0.42$, $P < 0.001$; Figure 3d) and N₂O ($0.14 < R^2 < 0.24$, $P < 0.005$; Figure 3f) were negatively correlated. During the study period, the soil CO₂ and N₂O fluxes of all forest types showed a significant exponential relationship with T₁₀ ($P < 0.001$), the coefficient of variation of the regression model ranged between 0.22 and 0.89. The Q₁₀ values of CO₂ fluxes in LF, PF, and BF were 5.47, 3.67, and 4.06, while those for N₂O were 2.23, 1.82, and 1.49, respectively.

The Person's correlation analysis between the greenhouse gas fluxes and various environmental factors is showed in Table 3. Three forest-type soil CO₂ fluxes had a significant negative correlation with TN ($P < 0.05$). The soil CH₄ fluxes exhibited significant correlation with TOC in LF and BF ($P < 0.01$) and had a significant positive correlation with TN in LF ($P < 0.05$). The soil N₂O fluxes showed a significant positive correlation with NH₄⁺-N and NO₃⁻-N in LF, NO₃⁻-N in PF ($P < 0.05$), and significant positive correlation with soil pH, NO₃⁻-N and TN in BF ($P < 0.01$).

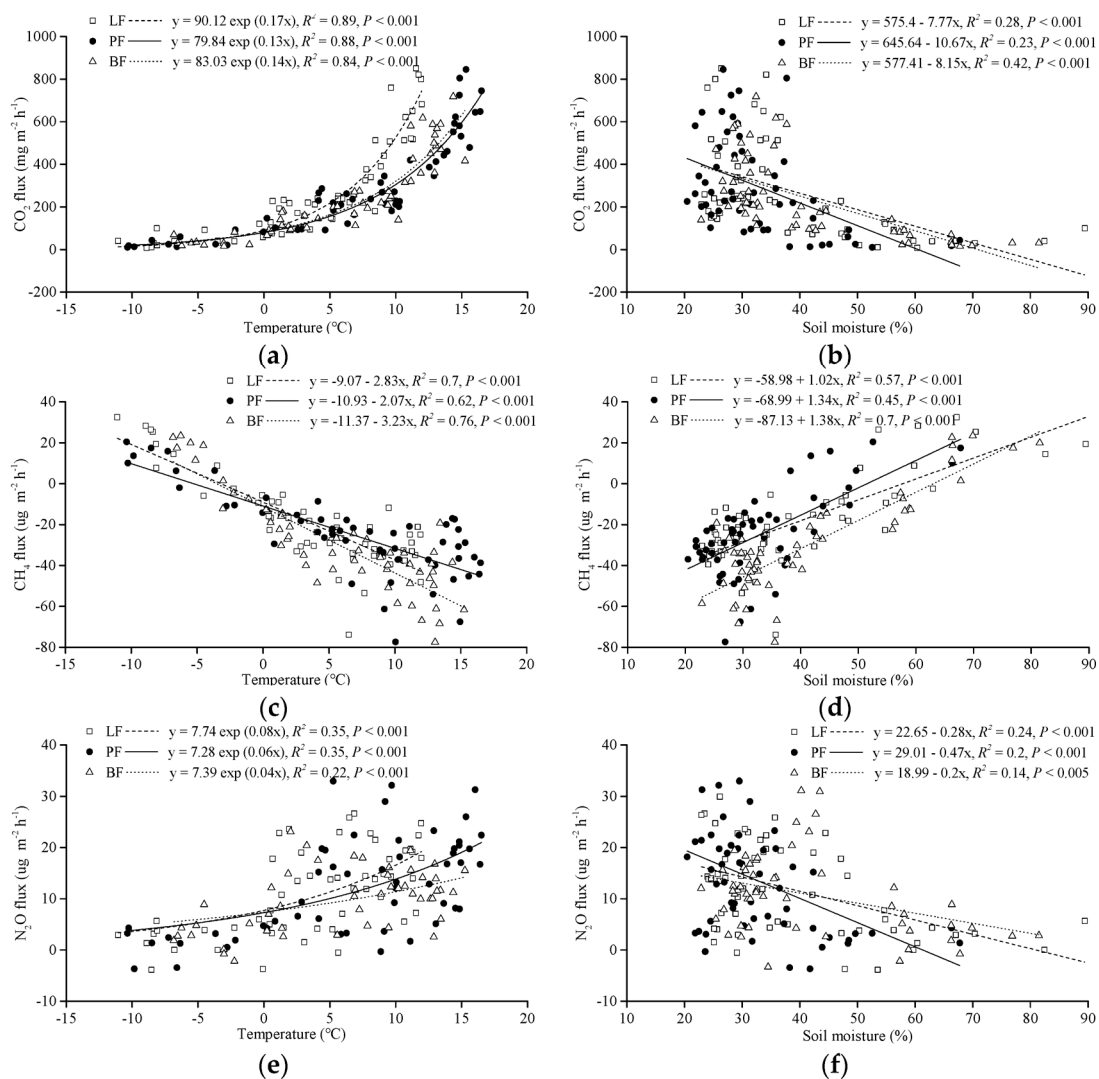


Figure 3. Relationships between (a) CO₂ fluxes and soil temperature, (b) CH₄ fluxes and soil temperature, (c) N₂O fluxes and soil temperature, (d) CO₂ fluxes and soil moisture, (e) CH₄ fluxes and soil moisture, and (f) N₂O fluxes and soil moisture in LF, PF, and BF.

Table 3. Relationship between greenhouse gas fluxes and soil physical and chemical properties in LP, PF, and BF.

Blocks	Flux	pH	NO ₃ ⁻ -N (mg·kg ⁻¹)	NH ₄ ⁺ -N (mg·kg ⁻¹)	TN (g·kg ⁻¹)	TOC (g·kg ⁻¹)
LF	CO ₂	0.235	-0.311	-0.234	-0.459 *	0.163
	CH ₄	0.236	-0.143	-0.318	0.471 *	-0.559 **
	N ₂ O	-0.336	0.444 *	0.549 **	-0.104	0.200
PF	CO ₂	-0.095	-0.228	-0.164	-0.506 *	0.411
	CH ₄	0.146	0.127	-0.133	0.202	-0.198
	N ₂ O	0.156	0.478 *	0.407	0.202	-0.044
BF	CO ₂	-0.409	-0.477 *	-0.168	-0.509 *	0.160
	CH ₄	0.122	-0.034	0.095	0.246	0.692 **
	N ₂ O	0.547 **	0.605 **	0.367	0.570 **	0.105

Note: ** Correlation is significant at the 0.01 level, * correlation is significant at the 0.05 level.

4. Discussion

4.1. Characteristics of Soil CO₂ Emissions from LF, PF, and BF

This study showed that the seasonal variation of CO₂ emission fluxes in typical forest LF, PF, and BF in the Daxing'an Mountains were similar, and reached a peak during the growing season (from July to August, Figure 2a), which is consistent with the results of the Song et al. [33] and Li et al. [34]. Soil CO₂ is mainly derived from autotrophic respiration (mainly vegetation root respiration), heterotrophic respiration (mainly soil microbial respiration), and mineralization decomposition of organic matter. The vegetation in this study area is mostly a shallow root system. During summer, with gradually increasing temperature, the appropriate combination of water and heat in the soil drives root respiration and soil microbial activity, which promotes soil CO₂ to reach emission peaks. Previous studies reported that the seasonal change of CO₂ emissions were dominant controlled by soil temperature [32,35]. This study found a consistent result, whereby soil temperature was significantly correlated with CO₂ fluxes as the dominant environmental variables in affect CO₂ emissions (Figure 3a). During the non-growing season, soil CO₂ fluxes fluctuated within a lower range. Analysis of the reasons indicated that root respiration and microbial activity were weak due to low temperature. On the other hand, when the soil was frozen, the active nutrient substrate, which can be directly used by microorganisms was reduced [36], thus resulting in the reduction of soil CO₂ fluxes. Two years of observations revealed that the temperature in the study area suddenly decreased due to the influence of low environment temperatures at the end of August each year, and the soil CO₂ fluxes of the three forest types decreased. Then, the soil CO₂ emission flux value increased, accompanying the increasing temperature back to the normal level of the same period [35]. This study found that the soil CO₂ fluxes in coniferous forests were higher than that in broad-leaved forests. The PF soil CO₂ cumulative fluxes were significantly higher than BF. Analysis of the reason found that the PF soil with high temperature had strong microbial metabolic activity, and the humus layer under the forest decomposed faster, releasing a large amount of CO₂ into the atmosphere. Q_{10} is widely used to assess the sensitivity of soil or ecosystem respiration to temperature changes [37]. The Q_{10} value of forest soil respiration in China is 1.33–5.53 [38]. The LF soil CO₂ fluxes ($Q_{10} = 5.47$) are more sensitive than BF ($Q_{10} = 4.06$) and PF ($Q_{10} = 3.67$) to temperature changes, which is consistent with the research results of Zheng et al. [39]. The significant correlation between soil temperature in the study area and soil CO₂ fluxes indicates strong positive short-term feedback between climate warming and soil CO₂ fluxes.

4.2. Characteristics of Soil CH₄ Emissions from LF, PF, and BF

CH₄ is produced by a biogeochemical cycle. It is oxidized by methanotrophs at the soil–water interface or rhizosphere aerobic environment, and the remainder is released into the atmosphere [40]. During this process, methanotrophs and methanogens play a key role. Previous studies have shown that soil CH₄ as trace gas has both absorption [41,42] and emission [43–45]. Soil hydrothermal conditions directly or indirectly change the community characteristics of anaerobic methanogens and aerobic methanotrophs to affect soil CH₄ fluxes; therefore, the difference in hydrothermal conditions under different ecosystems leads to different soil CH₄ fluxes [46]. This study observed that the three types of forest soil CH₄ showed overall absorption. Soil CH₄ emission, with maximum emission fluxes, only occurred in winter (January or February), and the other seasons showed absorption with the maximum absorption fluxes appearing in June (Figure 2b). After the soil was completely frozen in winter, the soil formed a better anaerobic environment, which was beneficial for the metabolic activity of methanogens and promoted the release of CH₄. At the beginning of the growing season, the thickness of the permafrost active layer further increases with increasing temperature, which provides a large place for the survival of the methanotrophs [47]. The release of C and N from the frozen microorganisms that were killed in winter provides an important matrix for methanotrophs to accelerate the oxidative absorption of CH₄ [48]. At the same time, the soil has a short drought period before the rainy season, which is conducive for the spread of atmospheric CH₄ and O₂ to the soil and increase the absorption of

CH₄ [49]. During summer, the soil moisture increases due to precipitation, and the soil CH₄ absorption decreases. The study also found that soil temperature and moisture were significantly related to soil CH₄ fluxes (Figure 3b,e). Soil CH₄ average annual absorption flux of three forest types showed BF > PF > LF, and the soil CH₄ absorption fluxes in the broad-leaved forest were higher than in the coniferous forest, which was consistent with the results of Steudler et al. [50]. The reason for this could be that LF and PF are loamy soils, which are tight and have poor aeration, while the soil bulk density of BF is relatively small, and the gravel content is high. The BF loose soil is conducive to oxygen transport, which enhances the activity of methane oxidase and methane oxidizing microorganisms in soil, which improves the absorption capacity of CH₄ in BF soil.

4.3. Characteristics of Soil N₂O Emissions from LF, PF, and BF

Soil nitrification and denitrification are two important links in the nitrogen cycle of ecosystems and form an important source of atmospheric N₂O. The monitoring results showed that N₂O fluxes of the three forest types were all sources of emissions. In June (during the growing season), soil N₂O fluxes showed peak emission periods. Thomas et al. [51] also reached a similar conclusion. The main reason may be that the outer surface of the soil particles is covered by an ice layer and the inner layer is wrapped with a tightly bound liquid water film, which forms a better anaerobic environment and remains high active nutrients after the soil completely frozen in winter [52]. The anaerobic environment provides a good place for denitrification to produce N₂O, which is sequestered by the frozen soil [53]. The N₂O enclosed in the soil is burst out into the atmosphere after thawing. In summer, plants grow vigorously and absorb a large amount of nitrogen. Competition between vegetation and microbes causes soil microbes to utilize substrate reduction, and frequent rainfall during the summer causes the shallow soil to alternate between wet and dry conditions, all of which affects the soil N₂O emission rate [54]. Permafrost soils, which are characterized by cold temperatures, have low net N mineralization rates and availability of mineral nitrogen [36]. Consequently, the available nitrogen in the soil (predominantly ammonium nitrogen and nitrate nitrogen) is poor in the forests of northern China [55]. This study found that PF soil N₂O fluxes were higher than LF and BF. The available nitrogen (NH₄⁺-N and NO₃⁻-N) contents of different forest types showed that BF was significantly higher than both PF and LF ($P < 0.05$), and the NH₄⁺-N content was significantly higher than the NO₃⁻-N content ($P < 0.05$) (Table 1). Therefore, denitrification may be the main source of soil N₂O fluxes in this region. However, BF soil pH was significantly lower than LF and PF ($P < 0.05$) (Table 1). According to Struwe et al. [56], the optimal pH range for denitrification in soil is between 6 and 8. Soil denitrification is inhibited under acidic conditions and the rate of denitrification decreases with increasing soil acidity. Therefore, the N₂O emission rate of LF was lower than that of PF and BF. Our study found that the temperature sensitivity of N₂O in LF, PF, and BF were 2.23, 1.82, and 1.49, respectively, and LF soil N₂O responded most to temperature rise. However, the difference of N₂O fluxes between the three forest types were not significant, and the forest type was not the main factor affecting soil N₂O fluxes.

5. Conclusions

- (1) The typical forest soil of the Daxing'an Mountains permafrost region was a "source" of CO₂ and N₂O and a "sink" of CH₄. The three greenhouse gas fluxes showed strong temporal variety, while the fluxes varied depending on the different sites. The PF soil CO₂ fluxes were significantly higher than BF. At the same time, the soil absorption fluxes of CH₄ in BF were significantly higher than that in LF.
- (2) Soil temperature and moisture were key environmental factors that correlated the CO₂ and CH₄ fluxes of different forest types in this high-latitude permafrost region. Q_{10} values showed that LF soil greenhouse gas fluxes were more sensitive to temperature. The N₂O fluxes were mainly correlated by the soil nitrogen content.
- (3) Against the background of climate warming, the CO₂ and N₂O emission rates of the three forest types increased with increasing temperature, and the CH₄ absorption rate decreased,

thus enhancing the atmospheric greenhouse effect. On a 100-year time scale, the greenhouse gas GWP of the three forest soil systems in the Daxing'an Mountains permafrost region was positive, which had positive feedback on global warming.

The Daxing'an Mountains permafrost region is extremely sensitive to climate change. The CO₂, CH₄, and N₂O fluxes in the study area had significant emission potential. Temperature alteration leads to complex changes in hydrothermal conditions that either directly or indirectly affect forest ecosystems in the cold region, which transforms ground-gas exchange ratios to affect greenhouse gas fluxes. In the future, stable isotope tracing and microbial high-throughput sequencing technologies will be comprehensively used to analyze the mechanism of soil greenhouse gas accumulation, conversion, and transmission in permafrost region.

Author Contributions: X.W., S.Z. and D.M. designed the experiment; X.W. and X.D. carried out the experiment; X.W. analyzed the data and wrote the manuscript; J.R. and Q.C. provided theory assistance and revised the manuscript.

Funding: This work was founded by the National Natural Science Foundation of China, grant number 41571199, 41501065, 41601382 and Doctorial Innovation Fund, grant number HSDBSCX 2019-02.

Acknowledgments: The authors sincerely thank the Mohe Forest Ecosystem National Positioning Observation and Research Station in Heilongjiang province for its support in this experiment, and sincerely appreciate the reviewers for their helpful comments to improve the manuscript.

Conflicts of Interest: The authors declare no conflict of interest.

References

1. IPCC. Climate Change 2014: Synthesis report. In *Contribution of Working Groups I, II and III to the Fifth Assessment Report of the Intergovernmental Panel on Climate Change*; Core Writing Team, Pachauri, R.K., Meyer, L.A., Eds.; IPCC: Geneva, Switzerland, 2014; p. 18.
2. Subhash, B. Paris agreement on Climate change: A booster to enable sustainable global development and beyond. *Int. J. Environ. Res. Pub. Health* **2016**, *13*, 1134.
3. WMO. *The State of Greenhouse Gases in the Atmosphere Based on Global Observations through 2017*; WMO: Geneva, Switzerland, 2018.
4. IPCC. Climate change 2007: The physical scientific basis. In *Contribution of Working Groups 1 to the Fourth Assessment Report of the Intergovernmental Panel on Climate Change*; Cambridge University Press: Cambridge, UK; New York, NY, USA, 2007; p. 104.
5. Yu, G.R.; Ren, W.; Chen, Z.; Zhang, L.M.; Wang, Q.F.; Wen, X.F.; He, N.P.; Zhang, L.; Fang, H.J.; Zhu, X.J.; et al. Construction and progress of Chinese terrestrial ecosystem carbon, nitrogen and water fluxes coordinated observation. *J. Geogr. Sci.* **2016**, *26*, 803–826.
6. Jorgenson, M.T.; Osterkamp, T.E. Response of boreal ecosystems to varying modes of permafrost degradation. *Can. J. Forest Res.* **2005**, *35*, 2100–2111. [[CrossRef](#)]
7. Harden, J.W.; Koven, C.D.; Ping, C.L.; Hugelius, G.; Mcguire, A.D.; Camill, P.; Jorgenson, T.; Kuhry, P.; Michaelson, G.J.; O'Donnell, J.A.; et al. Field information links permafrost carbon to physical vulnerabilities of thawing. *Geophys. Res. Lett.* **2012**, *39*, 51–60. [[CrossRef](#)]
8. Ozlu, E.; Kumar, S. Response of surface GHG fluxes to long-term manure and inorganic fertilizer application in corn and soybean rotation. *Sci. Total Environ.* **2018**, *626*, 817–825. [[CrossRef](#)]
9. Schuur, E.A.G.; McGuire, A.D.; Schadel, C.; Grosse, G.; Harden, J.W.; Hayes, D.J.; Hugelius, G.; Koven, C.D.; Kuhry, P.; Lawrence, D.M.; et al. Climate change and the permafrost carbon feedback. *Nature* **2015**, *520*, 171–179. [[CrossRef](#)]
10. Pan, Y.D.; Birdsey, R.A.; Fang, J.Y.; Houghton, R.; Kauppi, P.E.; Kurz, W.A.; Phillips, O.L.; Shvidenko, A.; Lewis, S.L.; Canadell, J.G.; et al. A large and persistent carbon sink in the world's forests. *Science* **2011**, *333*, 988–993.
11. Livesley, S.J.; Kiese, R.; Miehle, P.; Weston, C.J.; Butterbach-bahl, K.; Arndt, S.K. Soil-atmosphere exchange of greenhouse gases in a Eucalyptus marginata woodland, a clover-grass pasture, and Pinus radiata and Eucalyptus globulus plantations. *Glob. Chang. Biol.* **2009**, *15*, 425–440. [[CrossRef](#)]

12. Jang, I.; Lee, S.; Hong, J.H.; Kang, H. Methane oxidation rates in forest soils and their controlling variables: A review and a case study in Korea. *Ecol. Res.* **2006**, *21*, 849–854. [[CrossRef](#)]
13. Ju, H.; Shen, G.Z.; Xu, W.T.; Zhao, C.M.; Su, L.; Wang, Y.; Xie, Z.Q.; Zhang, Q.L. The emission of CH₄, CO₂, and N₂O in the typical forest soils of Shennongjia under the precipitation reduction. *Acta Ecol. Sin.* **2016**, *36*, 6397–6408.
14. Leckie, S.E.; Prescott, C.E.; Grayston, S.J. Forest floor microbial community response to tree species and fertilization of regenerating coniferous forests. *Can. J. Forest Res.* **2004**, *34*, 1426–1435. [[CrossRef](#)]
15. Wang, H.; Liu, S.R.; Mo, J.M.; Zhang, T. Soil-atmosphere exchange of greenhouse gases in subtropical plantations of indigenous tree species. *Plant Soil* **2010**, *335*, 213–227. [[CrossRef](#)]
16. Castro, M.S.; Steudler, P.A.; Melillo, J.M.; Aber, J.D.; Bowden, R.D. Factors controlling atmospheric methane consumption by temperate forest soils. *Glob. Biogeochem. Cycles* **1995**, *9*, 1–10. [[CrossRef](#)]
17. Butterbach-Bahl, K.; Gasche, R.; Willibald, G.; Papen, H. Exchange of N-gases at the HÖglwald forest-A summary. *Plant Soil* **2002**, *240*, 117–123. [[CrossRef](#)]
18. Gao, W.F.; Yao, Y.L.; Liang, H.; Song, L.Q.; Sheng, H.C.; Cai, T.J.; Gao, D.W. Emissions of nitrous oxide from continuous permafrost region in the Daxing'an Mountains, Northeast China. *Atmos. Environ.* **2019**, *198*, 34–45. [[CrossRef](#)]
19. Qing, D.H.; Yao, T.D.; Ding, Y.J.; Ren, J.W. *Cryospheric Sciences*, 1st ed.; Science Press: Beijing, China, 2017; pp. 49–55.
20. Zhou, Y.W.; Guo, D.X.; Qiu, G.Q.; Cheng, G.D.; Li, S.D. *Geocryology in China*, 1st ed.; Science Press: Beijing, China, 2000; pp. 40–42.
21. Yang, X.; Meng, J.; Lan, Y.; Chen, W.F.; Yang, T.X.; Yuan, J.; Liu, A.N.; Han, J. Effects of maize stover and its biochar on soil CO₂ emissions and labile organic carbon fractions in Northeast China. *Agr. Ecosyst. Environ.* **2017**, *240*, 24–31. [[CrossRef](#)]
22. Nie, T.Z.; Chen, P.; Zhang, Z.X.; Qi, Z.J.; Lin, Y.Y.; Xu, D. Effects of different types of water and nitrogen fertilizer management on greenhouse gas emissions, yield, and water consumption of paddy fields in cold region of China. *Int. J. Environ. Res. Pub. Health* **2019**, *16*, 1639. [[CrossRef](#)]
23. Song, C.C.; Wang, Y.S.; Wang, Y.Y.; Zhao, Z.C. Emission of CO₂, CH₄ and N₂O from freshwater marsh during freeze-thaw period in Northeast of China. *Atmos. Environ.* **2006**, *40*, 6879–6885. [[CrossRef](#)]
24. Cui, Q.; Song, C.C.; Wang, X.W.; Shi, F.X.; Yu, X.Y.; Tan, W.W. Effects of warming on N₂O fluxes in a boreal peatland of Permafrost region, Northeast China. *Sci. Total Environ.* **2018**, *616–617*, 427–434. [[CrossRef](#)]
25. Song, X.Y.; Wang, G.X.; Ran, F.; Chang, R.Y.; Song, C.L.; Xiao, Y. Effects of topography and fire on soil CO₂ and CH₄ flux in boreal forest underlain by permafrost in northeast China. *Ecol. Eng.* **2017**, *106*, 35–43. [[CrossRef](#)]
26. Stenberg, M.; Aronsson, H.; Lindén, B.; Rydberg, T.; Gustafson, A. Soil mineral nitrogen and nitrate leaching losses in soil tillage systems combined with a catch crop. *Soil Till. Res.* **1999**, *50*, 115–125. [[CrossRef](#)]
27. Reis, B.F.; Zagatto, E.A.G.; Javcintho, A.O.; Krug, F.J.; Bergamin, F.H. Merging zones in flow injection analysis: Part 4. Simultaneous spectrophotometric determination of total nitrogen and phosphorus in plant material. *Anal. Chim. Acta.* **1980**, *119*, 305–311. [[CrossRef](#)]
28. Franzluebbers, A.J.; Stuedemann, J.A. Particulate and non-particulate fractions of soil organic carbon under pastures in the Southern Piedmont USA. *Environ. Pollut.* **2002**, *116*, S53–S62. [[CrossRef](#)]
29. Song, C.C.; Xu, X.F.; Tian, H.Q.; Wang, Y.Y. Ecosystem-atmosphere exchange of CH₄ and N₂O and ecosystem respiration in wetlands in the Sanjiang Plain, Northeastern China. *Glob. Chang. Biol.* **2009**, *15*, 692–705. [[CrossRef](#)]
30. Peichl, M.; Arain, M.A.; Ullah, S.; Moore, T.R. Carbon dioxide, methane, and nitrous oxide exchanges in an age-sequence of temperate pine forests. *Glob. Chang. Biol.* **2010**, *16*, 2198–2212. [[CrossRef](#)]
31. Boone, R.D.; Nadelhoffer, K.J.; Canary, J.D.; Kaye, J.P. Roots exert a strong influence on the temperature sensitivity of soil respiration. *Nature* **1998**, *396*, 570–572. [[CrossRef](#)]
32. Jiang, C.M.; Yu, G.R.; Fang, H.J.; Cao, G.M.; Li, Y.N. Short-term effect of increasing nitrogen deposition on CO₂, CH₄ and N₂O fluxes in an alpine meadow on the Qinghai-Tibetan Plateau, China. *Atmos. Environ.* **2010**, *44*, 2920–2926. [[CrossRef](#)]
33. Song, X.Y.; Wang, G.X.; Hu, Z.Y.; Ran, F.; Chen, X.P. Boreal forest soil CO₂ and CH₄ fluxes following fire and their responses to experimental warming and drying. *Sci. Total Environ.* **2018**, *644*, 862–872. [[CrossRef](#)]

34. Li, Y.Y.; Dong, S.K.; Liu, S.L.; Zhou, H.K.; Gao, Q.Z.; Cao, G.G.; Wang, X.X.; Su, X.K.; Zhang, Y.; Tang, L.; et al. Seasonal changes of CO₂, CH₄ and N₂O fluxes in different types of alpine grassland in the Qinghai-Tibetan Plateau of China. *Soil Biol. Biochem.* **2015**, *80*, 306–314. [[CrossRef](#)]
35. Saito, M.; Kato, T.; Tang, Y. Temperature controls ecosystem CO₂ exchange of an alpine meadow on the northeastern Tibetan Plateau. *Glob. Chang. Biol.* **2009**, *15*, 221–228. [[CrossRef](#)]
36. Siciliano, S.D.; Ma, W.K.; Ferguson, S.; Farrell, R.E. Nitrifier dominance of Arctic soil nitrous oxide emissions arises due to fungal competition with denitrifiers for nitrate. *Soil Biol. Biochem.* **2009**, *41*, 1104–1110. [[CrossRef](#)]
37. Davidson, E.A.; Janssens, I.A. Temperature sensitivity of soil carbon decomposition and feedbacks to climate change. *Nature* **2006**, *440*, 165–173. [[CrossRef](#)] [[PubMed](#)]
38. Chen, G.S.; Yang, Y.S.; Lv, P.P.; Zhang, Y.P.; Qiang, X.L. Regional patterns of soil respiration in China's forests. *Acta Ecol. Sin.* **2008**, *28*, 1748–1761.
39. Zheng, Z.M.; Yu, G.R.; Fu, Y.L.; Wang, Y.S.; Sun, X.M.; Wang, Y.H. Temperature sensitivity of soil respiration is affected by prevailing climatic conditions and soil organic carbon content: A trans-China based case study. *Soil Biol. Biochem.* **2009**, *41*, 1531–1540. [[CrossRef](#)]
40. Gleb, K.; Ernst-Detlef, S.; Alla, Y.; Alexander, K.; Evgeny, C.; Elizaveta, R. Cryogenic displacement and accumulation of biogenic methane in frozen soils. *Atmosphere* **2017**, *8*, 105.
41. Zhang, L.H.; Hou, L.Y.; Guo, D.F.; Li, L.H.; Xu, X.F. Interactive impacts of nitrogen input and water amendment on growing season fluxes of CO₂, CH₄, and N₂O in a semiarid grassland, Northern China. *Sci. Total Environ.* **2016**, *10*, 523–535. [[CrossRef](#)]
42. Johnson, M.S.; Webster, C.; Jassal, R.S.; Hawthorne, L.; Black, T.A. Biochar influences on soil CO₂ and CH₄ fluxes in response to wetting and drying cycles for a forest soil. *Sci. Rep.* **2017**, *7*, 6780. [[CrossRef](#)] [[PubMed](#)]
43. Heimann, M. Atmospheric science: Enigma of the recent methane budget. *Nature* **2011**, *476*, 157–158. [[CrossRef](#)]
44. Cooper, M.D.A.; Estop-Aragonés, C.; Fisher, J.P.; Thierry, A.; Garnett, M.H.; Charman, D.J.; Murton, J.B.; Phoenix, G.K.; Treharne, R.; Kokeij, S.V.; et al. Limited contribution of permafrost carbon to methane release from thawing peatlands. *Nat. Clim. Chang.* **2017**, *7*, 507–511. [[CrossRef](#)]
45. Nie, T.Z.; Zhang, Z.X.; Qi, Z.J.; Chen, P.; Sun, Z.Y.; Liu, X.C. Characterizing spatiotemporal dynamics of CH₄ fluxes from rice paddies of cold region in Heilongjiang province under climate change. *Int. J. Environ. Res. Pub. Health* **2019**, *16*, 692. [[CrossRef](#)] [[PubMed](#)]
46. Wagner, D.; Lipski, A.; Embacher, A.; Gattinger, A. Methane fluxes in permafrost habitats of the Lena Delta: Effects of microbial community structure and organic matter quality. *Environ. Microbiol.* **2005**, *7*, 1582–1592. [[CrossRef](#)] [[PubMed](#)]
47. Sun, X.X.; Song, C.C.; Wang, X.W.; Mao, R.; Guo, Y.D.; Lu, Y.Z. Effect of permafrost degradation on methane emission in wetlands: A review. *Acta Ecol. Sin.* **2011**, *31*, 5379–5386.
48. Schimel, J.P.; Clein, J.S. Microbial response to freeze-thaw cycles in tundra and taiga soils. *Soil Biol. Biochem.* **1996**, *28*, 1061–1066. [[CrossRef](#)]
49. Borken, W.; Davidson, E.A.; Savage, K.; Sundquist, E.T.; Steudler, P. Effect of summer throughfall exclusion, summer drought, and winter snow cover on methane fluxes in a temperate forest soil. *Soil Biol. Biochem.* **2006**, *38*, 1388–1395. [[CrossRef](#)]
50. Steudler, P.A.; Bowden, R.D.; Melillo, J.M.; Aber, J.D. Influence of nitrogen fertilization on methane uptake in temperate forest soils. *Nature* **1989**, *341*, 314–316. [[CrossRef](#)]
51. Thomas, K.F.; Vern, S.B.; John, D.W.; John, A.B.; Raymonal, L.D.; Devon, W.; Reynald, L. Micrometeorological measurements reveal large nitrous oxide losses during spring thaw in Alberta. *Atmosphere* **2018**, *9*, 128.
52. Trotsenko, Y.A.; Khmelenina, V.N. Aerobic methanotrophic bacteria of cold ecosystems. *FEMS Microbiol. Ecol.* **2005**, *53*, 15–26. [[CrossRef](#)] [[PubMed](#)]
53. Teepe, R.; Brumme, R.; Beese, F. Nitrous oxide emissions from soil during freezing and thawing periods. *Soil Biol. Biochem.* **2001**, *33*, 1269–1275. [[CrossRef](#)]
54. Kuz'yakov, Y.; Xu, X.L. Competition between roots and microorganisms for nitrogen: Mechanisms and ecological relevance. *N. Phytol.* **2013**, *198*, 656–669. [[CrossRef](#)]

55. Luyssaert, S.; Schulze, E.D.; Börner, A.; Knohl, A.; Hessenmöller, D.; Law, B.E.; Ciais, P.; Grace, J. Old-growth forests as global carbon sinks. *Nature* **2008**, *455*, 213–215. [[CrossRef](#)]
56. Struwe, S.; Kjølter, A. Potential for N₂O production from beech (*Fagus silvatica*) forest soils with varying pH. *Soil Biol. Biochem.* **1994**, *26*, 1003–1009. [[CrossRef](#)]



© 2019 by the authors. Licensee MDPI, Basel, Switzerland. This article is an open access article distributed under the terms and conditions of the Creative Commons Attribution (CC BY) license (<http://creativecommons.org/licenses/by/4.0/>).